AGU ADVANCING EARTH AND SPACE SCIENCE

Geophysical Research Letters

RESEARCH LETTER
10.1029/2020GL090825

Key Points:
- The seasonal and regional transition to an ice-free Arctic is documented using CMIP6 models
- All Arctic shelf seas will be ice free in summer by the mid-2050s regardless of scenario
- The timing of ice-free conditions shows large regional and intermodel differences

Supporting Information:
- Table S1

Correspondence to:
M. Årthun,
marius.arthun@uib.no

Citation:
Årthun, M., Onarheim, I. H., Dörr, J., & Eldevik, T. (2021). The seasonal and regional transition to an ice-free Arctic. *Geophysical Research Letters*, *48*, e2020GL090825. https://doi.org/10.1029/2020GL090825

Received 14 SEP 2020
Accepted 19 NOV 2020

The Seasonal and Regional Transition to an Ice-Free Arctic

Marius Årthun[1], Ingrid H. Onarheim[2], Jakob Dörr[1], and Tor Eldevik[1]

[1]Geophysical Institute, University of Bergen and Bjerknes Centre for Climate Research, Bergen, Norway, [2]Equinor ASA, Bergen, Norway

Abstract The Arctic sea ice cover is currently retreating and will continue its retreat in a warming world. However, the loss of sea ice is neither regionally nor seasonally uniform. Here, we present the first regional and seasonal assessment of future Arctic sea ice loss in CMIP6 models under low (SSP126) and high (SSP585) emission scenarios, thus spanning the range of future change. We find that Arctic sea ice loss—at present predominantly limited to the summer season—will under SSP585 take place in all regions and all months. The summer sea ice is lost in all the shelf seas regardless of emission scenario, whereas ice-free conditions in winter before the end of this century only occur in the Barents Sea. The seasonal transition to ice-free conditions is found to spread through the Atlantic and Pacific regions, with change starting in the Barents Sea and Chukchi Sea, respectively.

Plain Language Summary We examine current and future Arctic sea ice loss in the latest generation of global climate models (CMIP6) focusing on regional and seasonal variability. We find that, unlike today, future Arctic sea ice loss will take place in all regions and all seasons. All Arctic shelf seas will become ice free in summer even if we follow a low emission scenario. Although future sea ice loss also takes place in winter, only the Barents Sea becomes ice free in winter before the end of this century.

1. Introduction

The Arctic sea ice cover has decreased in all seasons and all regions since satellite observations started in 1979 (Comiso et al., 2017; Onarheim et al., 2018), serving as a visible manifestation of ongoing climate change (Serreze et al., 2007). These changes in sea ice cover potentially impact several aspects of climate in the Arctic and lower latitudes, including ocean circulation and hydrography (Sévellec et al., 2017; Timmermans et al., 2018), large-scale atmospheric circulation (Deser et al., 2015; Screen, 2017), and marine ecosystems (Wassmann et al., 2011). Loss of Arctic sea ice also has important societal and economic consequences, impacting for example, shipping and exploitation of resources (Emmerson & Lahn, 2012; Smith & Stephenson, 2013).

In a warming world, the Arctic sea ice cover is expected to continue its retreat (Davy & Outten, 2020; Notz et al., 2020; Sigmond et al., 2018). However, Arctic sea ice loss has not been—and is not expected to be in the future—spatially uniform. Sea ice conditions and associated drivers of variability differ substantially from region to region within the Arctic, and considering only pan-Arctic trends thus masks competing regional trends and makes the underlying drivers and implications difficult to ascertain (Close et al., 2015; Li et al., 2017). For the same reason, prediction skill is also highly regionally dependent (Dai et al., 2020; Day et al., 2014), and various regions contribute differently to large-scale atmospheric circulation anomalies (Screen, 2017).

Arctic sea ice loss is also not seasonally uniform. Whereas the overall pan-Arctic sea ice loss has been largest in summer, the winter trends are of the same magnitude in the southernmost regions, and particularly in the Barents Sea (Onarheim & Årthun, 2017; Onarheim et al., 2018). The different rates of sea ice retreat in different seasons amplify the range of the seasonal cycle and change the seasonal climate of the Arctic Ocean (Bintanja & Van der Linden, 2013; Steele & Dickinson, 2016).

To better predict the local implications of Arctic sea ice loss, it is essential to establish how the future evolution of Arctic sea ice cover will manifest seasonally and regionally. Hence, in this study, we use models from the CMIP6 archive (Eyring et al., 2016) to detail the seasonal and regional transition to an ice-free Arctic.

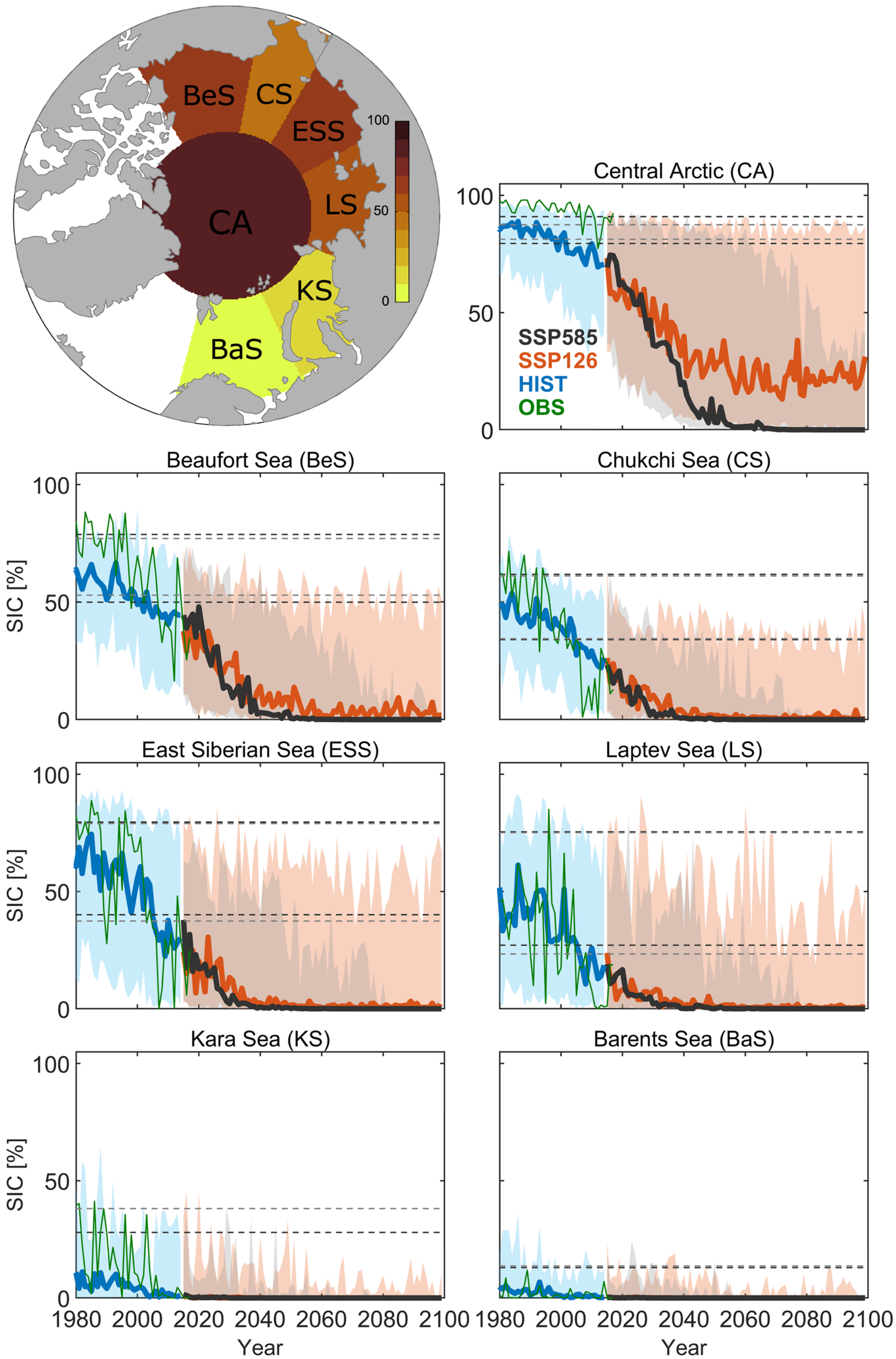
BeS
CS
ESS
LS
CA
KS
BaS
100
50
0
Central Arctic (CA)
SSP585
SSP126
HIST
OBS
Beaufort Sea (BeS)
Chukchi Sea (CS)
East Siberian Sea (ESS)
Laptev Sea (LS)
Kara Sea (KS)
Barents Sea (BaS)
SIC [%]
Year
1980 2000 2020 2040 2060 2080 2100

2. Data and Methods

To assess current and future regional and seasonal Arctic sea ice loss, we use monthly sea ice concentration (SIC; model variable *siconc*) from 19 models (see Table S1) from the CMIP6 archive (Eyring et al., 2016). The specific models were chosen based on the availability of SIC as output variable from both historical (years 1850–2014) simulations and future (2015–2100) simulations using the two Shared Socioeconomic Pathways (SSPs) scenarios SSP126 and SSP585 (Gidden et al., 2019). To avoid favoring a specific model in the results, we also restricted the selection of models to one per modeling center and use the first ensemble member for each model. The two future scenarios SSP126 and SSP585 represent a low-emission and a high-emission scenario, in which strong economic growth is fueled via sustainable and fossil fuel pathways, respectively (Gidden et al., 2019). Consequently, in SSP126, the radiative forcing decreases after 2050.

The focus of this study is on regional and seasonal sea ice loss in the Arctic and its shelf seas, that is, the Barents Sea, Kara Sea, Laptev Sea, East Siberian Sea, Chukchi Sea, and Beaufort Sea, in addition to the Central Arctic. Other seasonally ice-covered regions, such as the Canadian Archipelago, Greenland Sea, Bering Sea, and the Sea of Okhotsk, are not considered. We analyze changes in SIC, and not sea ice extent or area, as we compare sea ice loss in regions of different size.

We consider all months, but special emphasis is put on the difference between summer and winter, represented by September and March, respectively. To highlight future change, we calculate linear trends for three 30-year time periods: 1981–2010 (historical), 2021–2050 (near future), and 2070–2099 (end of the century). Time series are calculated on the models' native grid and the median and interquartile spread then calculated across the models.

We identify the first year with ice-free conditions for each month and region. Ice-free is defined as the first instance the area-averaged SIC falls below 15%. Our results are qualitatively similar for different definitions of ice-free conditions. To smooth out individual low sea ice years, ice-free years are identified based on 5-year low-pass-filtered data. SIC time series and trends are based on unfiltered data.

SIC trends from CMIP6 models are compared with satellite-derived observations between 1980 and 2017 (Walsh et al., 2019). The observations are available on a 0.25° latitude by 0.25° longitude grid. A comparison of regional sea ice trends in CMIP6 models with that in previous generation of climate models (CMIP5) is not performed here (see Davy and Outten [2020], Notz et al. [2020], and Shu et al. [2020] for a comparison of pan-Arctic sea ice extent/area).

To compare future sea ice loss with internal variability, we analyze preindustrial control simulations from the same 19 models. To obtain an estimate of the CMIP6-average internal variability, we average across the individual model spread (interdecile range; trend removed) using the last 400 years from each simulation. The CMIP6 estimate of internal variability is also compared with the (interdecile) spread across the 40 historical (1920–2005) simulations from the Community Earth System Model Large Ensemble (CESM-LE) (Kay et al., 2015).

3. Regional and Seasonal Evolution of Arctic Sea Ice

The evolution of regional summer and winter SIC is displayed in Figures 1 and 2, respectively. In the Arctic shelf seas, the summer sea ice is gradually lost in both emission scenarios. In the Central Arctic, the summer sea ice shows a strong decline for both scenarios but stabilizes at approximately 20% from around

Figure 1. Observed (OBS) and simulated time series of summer (September) sea ice concentration in different regions of the Arctic. The blue, red, and black lines show the ensemble median for the historical (HIST), SSP126, and SSP585 simulations, respectively, and the shading shows the interdecile spread. Dashed horizontal lines show the range of internal variability from CMIP6 preindustrial control simulations (black lines) and from historical CESM-LE simulations (gray lines). To enable easy comparison, both estimates of internal variability are plotted relative to the ensemble median HIST-SIC in 1980. The masks for the regional seas are shown in the map, color-coded by the loss of summer sea ice between 1980 and 2099 in SSP585. CESM-LE, Community Earth System Model Large Ensemble; SIC, sea ice concentration.

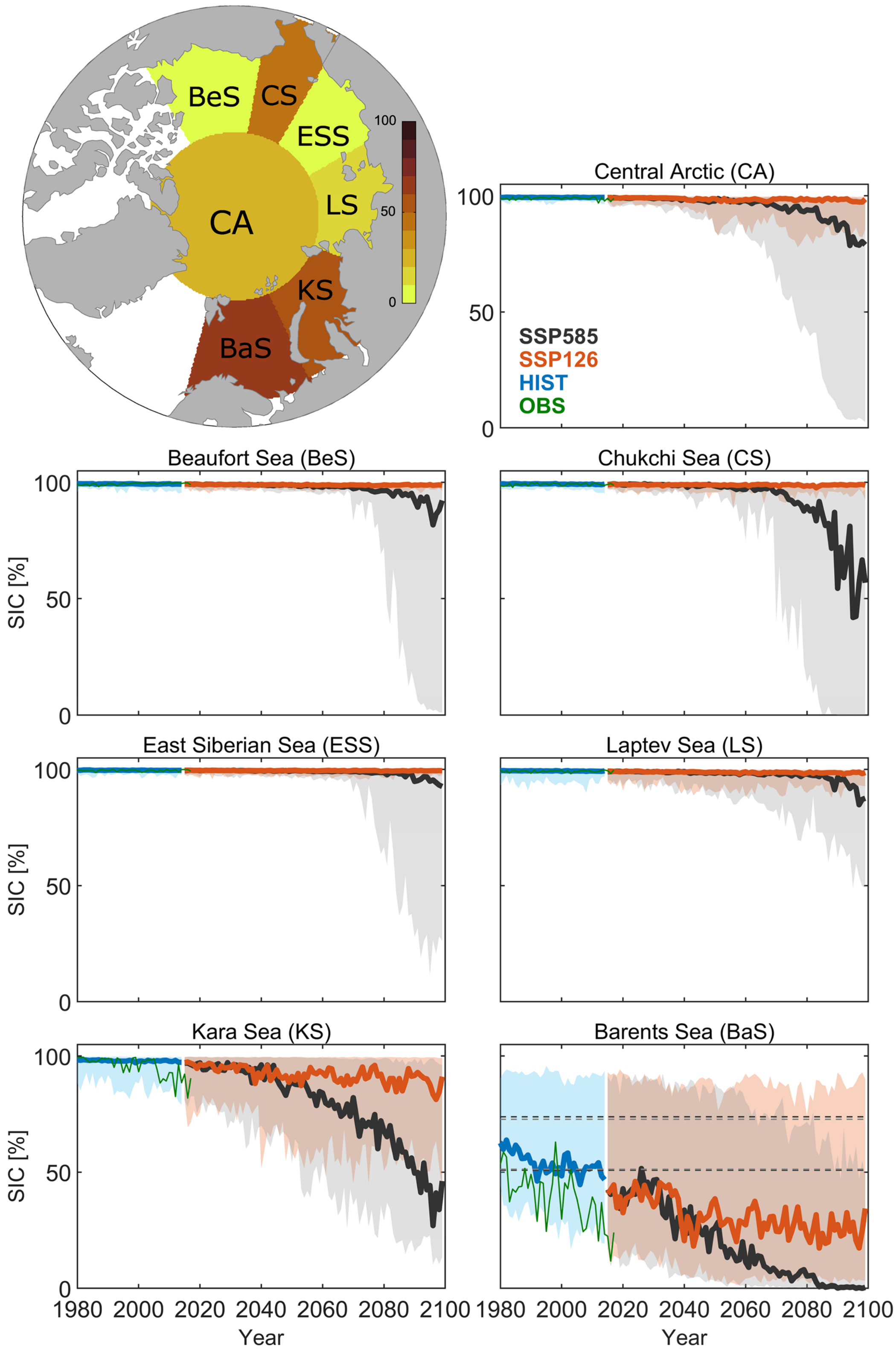
BeS
CS
ESS
LS
CA
KS
BaS
100
50
0
Central Arctic (CA)
SSP585
SSP126
HIST
OBS
Beaufort Sea (BeS)
Chukchi Sea (CS)
East Siberian Sea (ESS)
Laptev Sea (LS)
Kara Sea (KS)
Barents Sea (BaS)
SIC [%]
1980 2000 2020 2040 2060 2080 2100
Year

2060 under SSP126 (Figure 1). This new, stable state under SSP126 is also seen for pan-Arctic surface air temperature (Davy & Outten, 2020).

Future sea ice loss in winter extends over the whole Arctic in the high-emission scenario (Figure 2). The Kara and Barents Seas show a steady loss of winter sea ice throughout the century, whereas winter sea ice loss is more modest on the Pacific side, except for the Chukchi Sea which shows accelerating sea ice loss after around 2070. Under the SSP126 scenario, all Arctic regions display little future change in winter SIC, although there is a notable decline in the Barents and Kara Seas during the first few decades.

To further assess regional and seasonal sea ice change, we examine the SIC trends for each month and each region (Figures 3 and 4a–4g). As observed (1981–2010), recent Arctic sea ice loss in CMIP6 models is restricted to summer and early autumn, except for the Barents Sea where sea ice is lost also in the winter months. The simulated trends (ensemble median) are nevertheless typically smaller than the observed trends for all seasons and regions. The discrepancy is largest for the summer months (August–October) in the Chukchi and East Siberian Seas, where the simulated trends are, on average, 39% and 53%, respectively, of that observed (Figures 4c and 4d). For the Central Arctic, the simulated summer sea ice loss is larger than in observations. We note, however, that the area around the North Pole is not observed by the satellites (filled using the average of neighboring grid cells; Walsh et al., 2019) and that different observational products show significant disagreements in SIC (Comiso et al., 2017).

The weaker regional sea ice loss in CMIP6 models (ensemble median) than that observed is in line with that found for pan-Arctic sea ice extent trends in CMIP5 and CMIP3 models (Stroeve et al., 2012). However, trends calculated from the ensemble median only represent the externally forced sea ice loss, and, hence, does not include the impact of internal variability (Årthun et al., 2019; England et al., 2019; Notz et al., 2020). The intermodel spread is also substantial, and the observed trends are within the range of the model spread in all regions (Figures 4a–4g).

During the next few decades (2021–2050; Figures 3c and 3d), sea ice loss is projected to extend further into autumn/early winter (November–December) and spring (June). The Barents and Kara Seas have lost their summer sea ice and further retreat of the ice cover now takes place in winter. The ice-loss season is generally 2 months longer for SSP585 than for SSP126: 1 month longer in spring and 1 in winter. The trends are also, as expected, larger for the high-emission scenario.

Toward the end of the century (2070–2099), sea ice trends are small for SSP126 (Figure 3e). This is because sea ice either is gone (no more summer sea ice in the shelf seas) or further loss has been prevented by decreased emissions (as e.g., seen for the Central Arctic in summer and the Barents Sea in winter). For SSP585, sea ice loss takes place in winter in all regions, whereas trends are nonexistent (small) in the (practically) ice-free Arctic summer months (August–October; Figure 3f). The Arctic has thus completed the transition from a perennial to a seasonal sea ice cover, and the continued sea ice retreat is carried by winter.

Future sea ice loss is not seasonally symmetric centered on September but larger in autumn/winter (freezing season) than spring (melt season; Figure 3). This seasonal asymmetry in sea ice loss could be linked to a strong ocean thermal feedback and upper ocean warming in autumn in response to sea ice loss and ice-albedo feedback in summer (Stammerjohn et al., 2012; Steele & Dickinson, 2016), and enhanced wintertime atmospheric warming as a result of sea ice thinning (Labe et al., 2018; Lang et al., 2017). The faster future sea ice decline in autumn than in spring for the Chukchi and Beaufort Seas (Figure 3; Lebrun et al., 2019; Wang & Overland, 2015) could also be related to the seasonality of ocean heat transport through the Bering Strait (Serreze et al., 2016).

Figure 2. Observed (OBS) and simulated time series of winter (March) sea ice concentration in different regions of the Arctic. The blue, red, and black lines show the ensemble median for the historical (HIST), SSP126, and SSP585 simulations, respectively, and the shading shows the interdecile spread. Dashed horizontal lines show the range of internal variability from CMIP6 preindustrial control simulations (black lines) and from historical CESM-LE simulations (gray lines: only shown for the Barents Sea as preindustrial SIC is ~100% in the other shelf seas). To enable easy comparison, both estimates of internal variability are plotted relative to the ensemble median HIST-SIC in 1980. The masks for the regional seas are shown in the map, color-coded by the loss of winter sea ice between 1980 and 2099 in SSP585. CESM-LE, Community Earth System Model Large Ensemble; SIC, sea ice concentration.

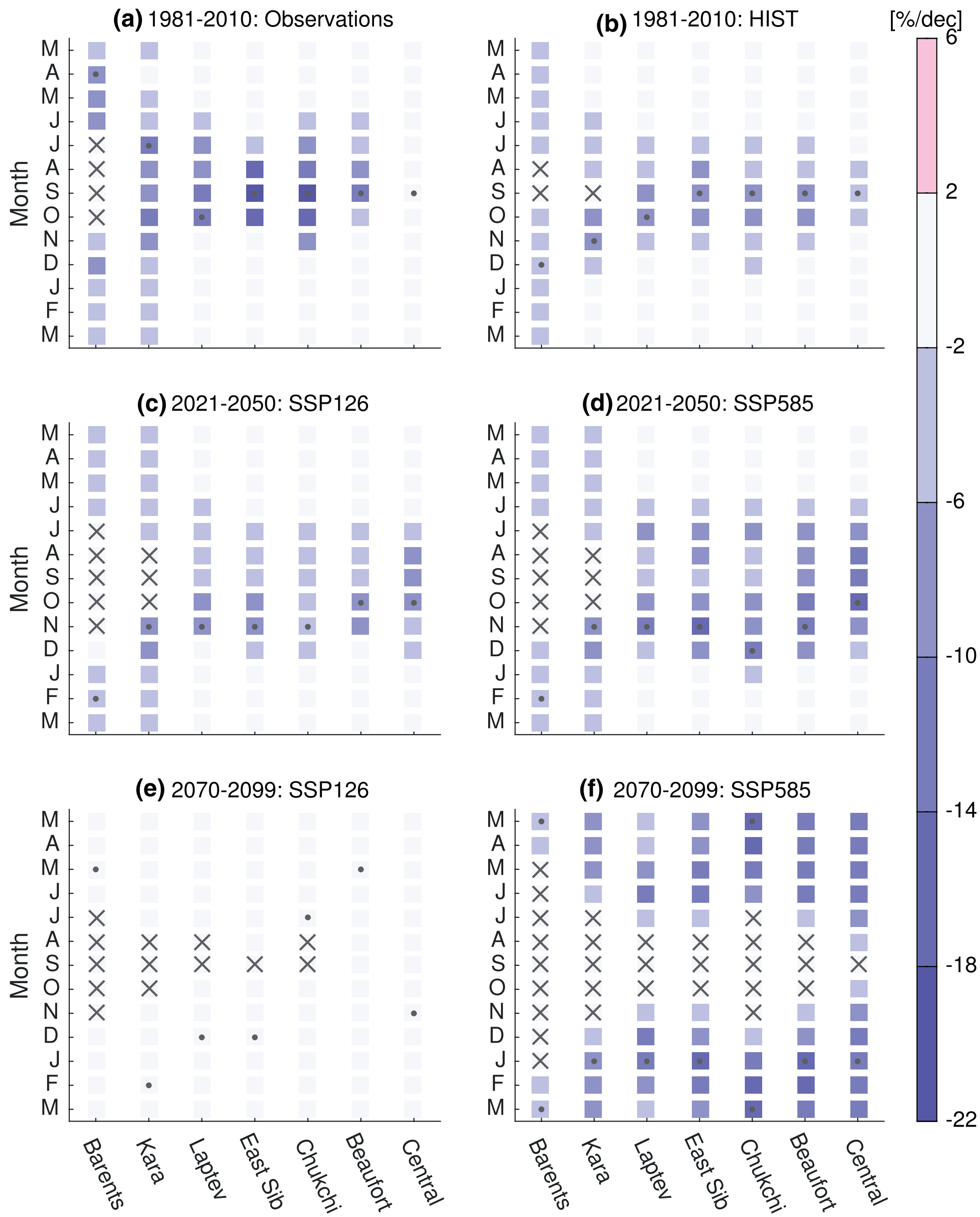

Figure 3. Regional and seasonal sea ice concentration trends for (a and b) observations and CMIP6 between 1981 and 2010, (c and d) 2021–2050 for SSP126 and SSP585, respectively, and (e and f) 2070–2099 for SSP126 and SSP585, respectively. Dots show months with maximum trend, while crosses indicate months that start with ice-free conditions (SIC below 15%). Simulated (CMIP6) trends are based on the ensemble median. The regions are ordered from left to right along the *x* axis in a counterclockwise direction through the Arctic Ocean, starting from the Barents Sea. On the *y* axis, months are ordered from March to March and centered on September. SIC, sea ice concentration.

4. Timing of an Ice-Free Arctic

Different rates of sea ice loss (Figure 3) lead to regional and seasonal differences in the timing of ice-free conditions (Figures 4h–4n). Under SSP126, the Arctic summer months (August–October) become ice free in all regions except for the Central Arctic (Figures 4h–4n). In the Kara Sea, ice-free months also include June and November, whereas in the Barents Sea, all months except February–April experience ice-free con-

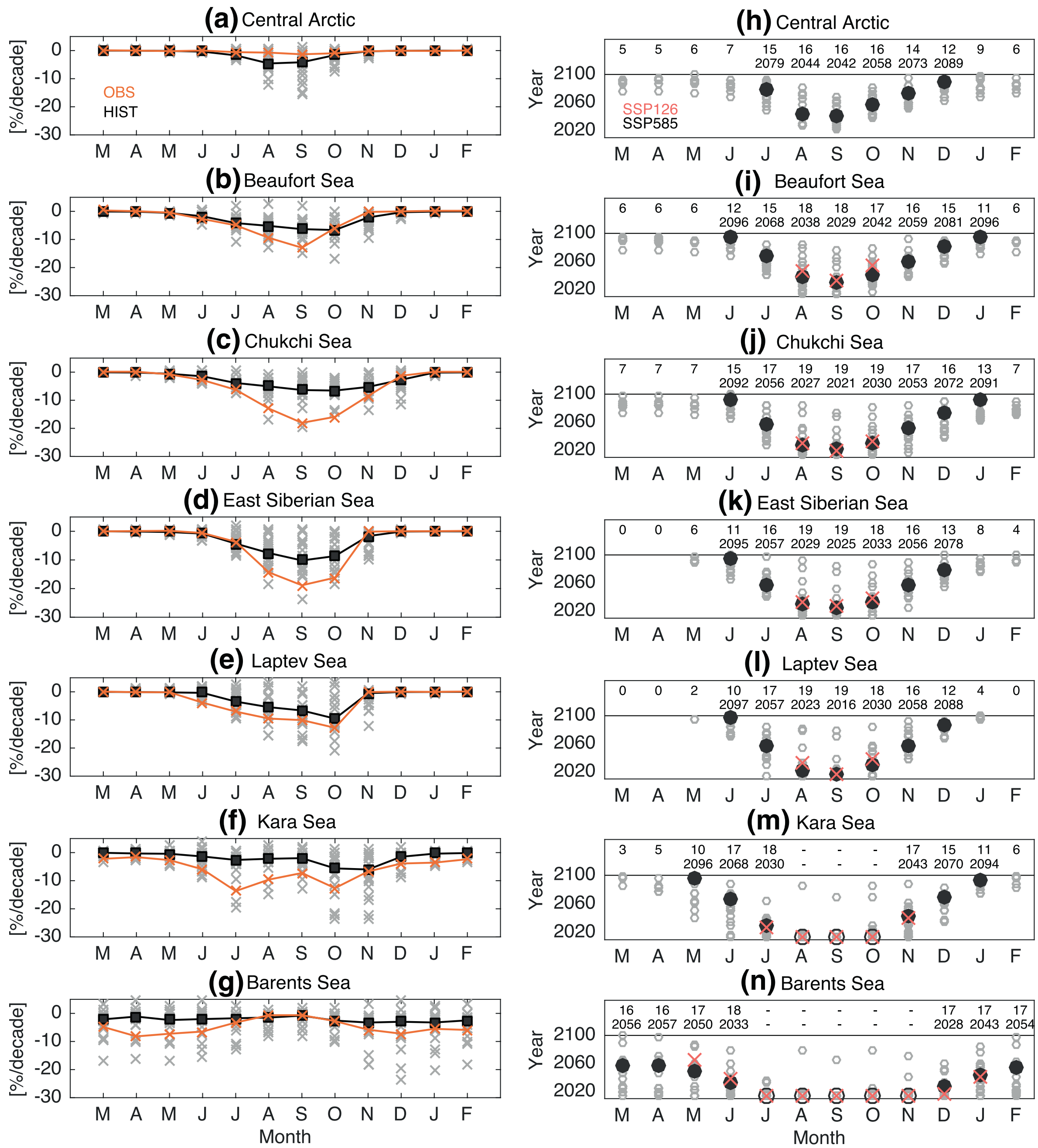

Figure 4. (a–g) Observed (OBS) and simulated (HIST) sea ice concentration trends between 1981 and 2010. Individual models are indicated by gray crosses and the ensemble median by black squares. (h–n) First year of ice-free conditions (SIC < 15%) in different regions and months. Black circles and red crosses show the timing of ice-free conditions for SSP585 and SSP126, respectively, based on the ensemble median SIC (for SSP585, the year is also listed in the panel above). Gray circles show the individual models that become ice free for SSP585 and the associated number of models is listed above. Months with ice-free conditions before 2015 are indicated by unfilled black circles and numbered by "–." On the *x*-axis, months are ordered from March to February and centered on September. SIC, sea ice concentration.

ditions in this century. Under SSP585, all shelf seas become ice free from June to December. The Barents Sea becomes ice-free year-round in the 2050s. Consistent with the seasonal asymmetric sea ice loss (Figure 3), ice-free conditions in the Chukchi and Beaufort Seas occur sooner in autumn than spring (Figures 4i and 4j). On the Atlantic side (Laptev, Kara, and Barents Seas), on the other hand, the timing of ice-free conditions is similar for the melt and freezing seasons.

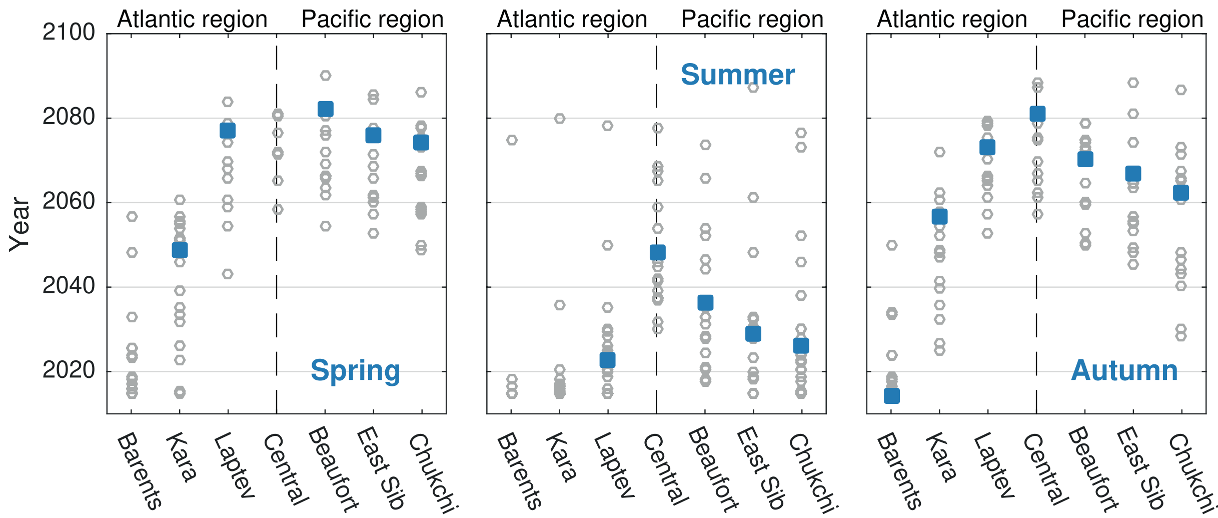

Figure 5. Regional variations in the timing of ice-free conditions (SIC < 15%) for spring (June–July), summer (August–October), and autumn (November–December) in SSP585. May and January are not included in spring and autumn, respectively, as fewer regions become ice free for these months. The filled blue squares represent the ensemble median, whereas the open gray circles show the individual models that become ice free. Missing values for the Barents and Kara Seas imply that these regions have been practically ice free (ensemble median) during these months also for historical time period. The regions along the *x*-axis are ordered looking toward the Central Arctic from the Barents and Chukchi Seas, representing the gateways to the Atlantic and Pacific regions, respectively. SIC, sea ice concentration.

The future loss of Arctic sea ice is seen to shift not only from summer to fall and then to winter but also from the peripheral shelf seas toward the Central Arctic (Figure 5). In the Atlantic sector, the occurrence of ice-free conditions progresses eastward, moving from the Barents Sea to the Kara and Laptev Seas. This pathway of change is consistent with the observed increasing intrusion of warm Atlantic waters into the Arctic, often referred to as an "Atlantification" of the Arctic (Årthun et al., 2012; Polyakov et al., 2017). Future projections show a sustained incursion of Atlantic waters into the Eurasian Basin throughout the century (Årthun et al., 2019), consistent with the slow eastward progression of ice-free conditions in the Atlantic region (Figure 5).

On the Pacific side, the loss of sea ice generally advances from the Chukchi Sea to the East Siberian and Beaufort Seas. Note that we are suggesting that both follow change in the Chukchi Sea, not that there is a link between sea ice loss in the East Siberian and Beaufort Seas. Consistent with the Chukchi Sea as a gatekeeper of downstream change, the observed warming of the Beaufort Gyre over the past three decades has been linked to ice loss and warming of surface waters in the Chukchi Sea (Timmermans et al., 2018). The delayed occurrence of ice-free conditions in the Beaufort Sea relative to the East Siberian Sea could be a result of sea ice convergence in the Beaufort Gyre and along the Alaskan/Canadian coast (Holland & Kimura, 2016). However, further investigation of regional drivers of sea ice loss—observed and simulated—is warranted to better understand the spatiotemporal differences in sea ice retreat identified here.

Our analysis provides valuable information about regional differences in future Arctic sea ice loss, which are not captured by pan-Arctic projections (Davy & Outten, 2020; Notz et al., 2020). It is nevertheless important to keep in mind that regional differences in, e.g., the timing of ice-free conditions also exist within the individual Arctic shelf seas (Close et al., 2015; Wang & Overland, 2015). In particular, there is for all seasons a clear latitudinal dependence, with the southern parts of the shelf seas generally becoming ice free earlier than the northern parts (not shown). The north-south gradient in sea ice loss is most pronounced for summer and spring, consistent with a strong latitudinal dependency of incoming shortwave radiation (Notz & Stroeve, 2016) and the influence of changes in solar heating on sea ice loss in the melt season (Stroeve et al., 2014). This further highlights that regional-scale differences are important to consider in the transition to an ice-free Arctic.

5. Discussion and Conclusions

In this study, we have presented the first regional and seasonal assessment of future Arctic sea ice loss. We find, using CMIP6 models, that Arctic sea ice loss—at present predominantly limited to the summer season—will in a high-emission scenario (SSP585) take place in all regions and all months. Ice-free conditions in winter before the end of this century only occur in the Barents Sea, which becomes ice-free year-round in the 2050s. The summer sea ice is lost in all the Arctic shelf seas regardless of emission scenario, and the timing of ice-free conditions are also practically the same (Figure 4).

Future sea ice loss and the projected timing of ice-free conditions display a substantial spread across the different models. For the shelf seas still presently ice covered in summer, the spread in future (SSP585) September sea ice loss is reflected in a 58–70-year prediction uncertainty of ice-free conditions, while the uncertainty is 46 years for the Central Arctic. The latter is consistent with recent findings from the CMIP5 Multi-Model Large Ensemble (Landrum & Holland, 2020). The identified spread in future SIC development is a result of large internal climate variability (Årthun et al., 2019; England et al., 2019) and because of model differences and biases (Ilıcak et al., 2016; Massonnet et al., 2012). As the shelf regions lie along the minimum summer sea-ice edge, they experience large internal variability that is comparable to the model spread (Figure 1). In contrast, the model spread for summer SIC in the Central Arctic is much larger than expected from internal variability alone, reflected in a larger prediction uncertainty than obtained from single model large ensembles (21 years) (Jahn et al., 2016). For winter (March) sea ice in the Barents Sea, the model spread (84 years; Figure 2) is also much larger than that associated with internal variability (27 years) (Onarheim & Årthun, 2017).

The prediction uncertainty associated with model biases can potentially be reduced by a subselection or weighting of models based on their agreement with observations (Knutti et al., 2017; Massonnet et al., 2012; Notz et al., 2020). Using only the eight models with a reasonable simulation of past Arctic sea ice conditions (Notz et al., 2020; Table S1), the spread in the timing of ice-free conditions is reduced (e.g., by 10 years for summer sea ice in the Central Arctic; note that a random subselection of eight models does not reduce the ensemble spread) and ice-free conditions occur earlier for all regions and seasons (e.g., the Barents Sea becoming ice-free year-round by 2038).

The timing of ice-free conditions furthermore shows large regional differences, generally moving poleward from the Barents and Chukchi Seas on the Atlantic and Pacific sides, respectively. As different seas are at different stages on their paths to ice-free conditions, this offers a possible "space-for-time" perspective on the evolution of regional Arctic sea ice cover (i.e., infer potential temporal changes from spatial gradients), which could translate into some potential in predicting the general development of sea ice conditions in one region based on previous change in another (Onarheim et al., 2018).

This work improves our understanding of future regional and seasonal Arctic sea ice loss. Previous multimodel assessments of Arctic sea ice have predominantly considered changes in pan-Arctic sea ice cover (Davy & Outten, 2020; Massonnet et al., 2012; Notz et al., 2020; Sigmond et al., 2018; Stroeve et al., 2012). However, as shown here, future sea ice change under anthropogenic warming has widely different regional and seasonal footprints, which are essential to examine as they have different impacts on the regional climate, ecosystem, and economy.

Data Availability Statement

The CMIP6 data used for this study are freely available from the Earth System Grid Federation (ESGF) (https://esgf-node.llnl.gov/search/cmip6). Data from the CESM-LE are available from http://www.cesm.ucar.edu/projects/community-projects/LENS/. Observed Arctic SICs are available from https://nsidc.org/data/G10010

Acknowledgments
This work received funding from the Research Council of Norway projects Nansen Legacy (grant 276730) and PATHWAY (grant 263223) and the Trond Mohn Foundation (grant BFS2018TMT01). We are grateful to all modeling centers for carrying out the CMIP6 simulations used here. We thank two anonymous reviewers for valuable comments that improved the manuscript and Richard Davy for help with obtaining the data.

References

Årthun, M., Eldevik, T., & Smedsrud, L. H. (2019). The role of Atlantic heat transport in future Arctic winter sea ice loss. *Journal of Climate*, *32*(11), 2603327–2603341.

Årthun, M., Eldevik, T., Smedsrud, L. H., Skagseth Ø., & Ingvaldsen, R. B. (2012). Quantifying the influence of Atlantic heat on Barents Sea ice variability and retreat. *Journal of Climate*, *25*, 4736–4743.

Bintanja, R., & Van der Linden, E. (2013). The changing seasonal climate in the Arctic. *Scientific Reports*, *3*(1), 1–8.

Close, S., Houssais, M.-N., & Herbaut, C. (2015). Regional dependence in the timing of onset of rapid decline in Arctic sea ice concentration. *Journal of Geophysical Research: Oceans*, *120*, 8077–8098. https://doi.org/10.1002/2015JC011187

Comiso, J. C., Meier, W. N., & Gersten, R. (2017). Variability and trends in the Arctic Sea ice cover: Results from different techniques. *Journal of Geophysical Research: Oceans*, *122*, 6883–6900. https://doi.org/10.1002/2017JC012768

Dai, P., Gao, Y., Counillon, F., Wang, Y., Kimmritz, M., & Langehaug, H. R. (2020). Seasonal to decadal predictions of regional Arctic sea ice by assimilating sea surface temperature in the Norwegian Climate Prediction Model. *Climate Dynamics*, *54*, 3863–3878.

Davy, R., & Outten, S. (2020). The Arctic surface climate in CMIP6: Status and developments since CMIP5. *Journal of Climate*, *33*(18), 8047–8068.

Day, J., Tietsche, S., & Hawkins, E. (2014). Pan-Arctic and regional sea ice predictability: Initialization month dependence. *Journal of Climate*, *27*(12), 4371–4390.

Deser, C., Tomas, R. A., & Sun, L. (2015). The role of ocean–atmosphere coupling in the zonal-mean atmospheric response to Arctic sea ice loss. *Journal of Climate*, *28*(6), 2168–2186.

Emmerson, C., & Lahn, G. (2012). *Arctic opening: Opportunity and risk in the high north*, (55). Lloyd's. Retrieved from http://library.arcticportal.org/1671/1/Arctic_Opening%2C_opportunity_and_risks_in_the_High_North.pdf

England, M., Jahn, A., & Polvani, L. (2019). Nonuniform contribution of internal variability to recent Arctic Sea ice loss. *Journal of Climate*, *32*(13), 4039–4053.

Eyring, V., Bony, S., Meehl, G. A., Senior, C. A., Stevens, B., Stouffer, R. J., & Taylor, K. E. (2016). Overview of the Coupled Model Intercomparison Project phase 6 (CMIP6) experimental design and organization. *Geoscientific Model Development*, *9*, 1937–1958.

Gidden, M., Riahi, K., Smith, S., Fujimori, S., Luderer, G., Kriegler, E., et al. (2019). Global emissions pathways under different socioeconomic scenarios for use in CMIP6: A dataset of harmonized emissions trajectories through the end of the century. *Geoscientific Model Development*, *12*(4), 1443–1475.

Holland, P. R., & Kimura, N. (2016). Observed concentration budgets of Arctic and Antarctic sea ice. *Journal of Climate*, *29*(14), 5241–5249.

Ilıcak, M., Drange, H., Wang, Q., Gerdes, R., Aksenov, Y., Bailey, D., et al. (2016). An assessment of the Arctic Ocean in a suite of interannual CORE-II simulations. Part III: Hydrography and fluxes. *Ocean Modelling*, *100*, 141–161.

Jahn, A., Kay, J. E., Holland, M. M., & Hall, D. M. (2016). How predictable is the timing of a summer ice-free Arctic? *Geophysical Research Letters*, *43*, 9113–9120. https://doi.org/10.1002/2016GL070067

Kay, J. E., Deser, C., Phillips, A., Mai, A., Hannay, C., Strand, G., et al. (2015). The Community Earth System Model (CESM) large ensemble project: A community resource for studying climate change in the presence of internal climate variability. *Bulletin of the American Meteorological Society*, *96*(8), 1333–1349.

Knutti, R., Sedláček, J., Sanderson, B. M., Lorenz, R., Fischer, E. M., & Eyring, V. (2017). A climate model projection weighting scheme accounting for performance and interdependence. *Geophysical Research Letters*, *44*, 1909–1918. https://doi.org/10.1002/2016GL072012

Labe, Z., Peings, Y., & Magnusdottir, G. (2018). Contributions of ice thickness to the atmospheric response from projected Arctic sea ice loss. *Geophysical Research Letters*, *45*, 5635–5642. https://doi.org/10.1029/2018GL078158

Landrum, L., & Holland, M. M. (2020). Extremes become routine in an emerging new Arctic. *Nature Climate Change*, *10*, 1108–1115.

Lang, A., Yang, S., & Kaas, E. (2017). Sea ice thickness and recent Arctic warming. *Geophysical Research Letters*, *44*, 409–418. https://doi.org/10.1002/2016GL071274

Lebrun, M., Vancoppenolle, M., Madec, G., & Massonnet, F. (2019). Arctic sea-ice-free season projected to extend into autumn. *The Cryosphere*, *13*, 79–96.

Li, D., Zhang, R., & Knutson, T. R. (2017). On the discrepancy between observed and CMIP5 multi-model simulated Barents Sea winter sea ice decline. *Nature Communications*, *8*, 14991.

Massonnet, F., Fichefet, T., Goosse, H., Bitz, C. M., Philippon-Berthier, G., Holland, M. M., & Barriat, P.-Y. (2012). Constraining projections of summer Arctic sea ice. *The Cryosphere*, *6*(6), 1383–1394.

Notz, D., Dörr, J., Bailey, D. A., Blockley, E., Bushuk, M., Debernard, J. B., et al. (2020). Arctic Sea ice in CMIP6. *Geophysical Research Letters*, *47*, e2019GL086749. https://doi.org/10.1029/2019GL086749

Notz, D., & Stroeve, J. (2016). Observed Arctic sea-ice loss directly follows anthropogenic CO_2 emission. *Science*, *354*(6313), 747–750.

Onarheim, I. H., & Årthun, M. (2017). Toward an ice-free Barents Sea. *Geophysical Research Letters*, *44*, 8387–8395. https://doi.org/10.1002/2017GL074304

Onarheim, I. H., Eldevik, T., Smedsrud, L. H., & Stroeve, J. C. (2018). Seasonal and regional manifestation of Arctic sea ice loss. *Journal of Climate*, *31*(12), 4917–4932.

Polyakov, I. V., Pnyushkov, A. V., Alkire, M. B., Ashik, I. M., Baumann, T. M., Carmack, E. C., et al. (2017). Greater role for Atlantic in flows on sea-ice loss in the Eurasian Basin of the Arctic Ocean. *Science*, *356*(6335), 285–291.

Screen, J. A. (2017). Simulated atmospheric response to regional and pan-Arctic sea ice loss. *Journal of Climate*, *30*(11), 3945–3962.

Serreze, M. C., Crawford, A. D., Stroeve, J. C., Barrett, A. P., & Woodgate, R. A. (2016). Variability, trends, and predictability of seasonal sea ice retreat and advance in the Chukchi Sea. *Journal of Geophysical Research: Oceans*, *121*, 7308–7325. https://doi.org/10.1002/2016JC011977

Serreze, M. C., Holland, M. M., & Stroeve, J. (2007). Perspectives on the Arctic's shrinking sea-ice cover. *Science*, *315*(5818), 1533–1536.

Sévellec, F., Fedorov, A. V., & Liu, W. (2017). Arctic sea-ice decline weakens the Atlantic Meridional Overturning Circulation. *Nature Climate Change*, *7*(8), 604–610.

Shu, Q., Wang, Q., Song, Z., Qiao, F., Zhao, J., Chu, M., & Li, X. (2020). Assessment of sea ice extent in CMIP6 with comparison to observations and CMIP5. *Geophysical Research Letters*, *47*, e2020GL087965. https://doi.org/10.1029/2020GL087965

Sigmond, M., Fyfe, J. C., & Swart, N. C. (2018). Ice-free Arctic projections under the Paris Agreement. *Nature Climate Change*, *8*(5), 404–408.

Smith, L. C., & Stephenson, S. R. (2013). New Trans-Arctic shipping routes navigable by midcentury. *Proceedings of the National Academy of Sciences*, *110*(13), E1191–E1195.

Stammerjohn, S., Massom, R., Rind, D., & Martinson, D. (2012). Regions of rapid sea ice change: An inter-hemispheric seasonal comparison. *Geophysical Research Letters*, *39*, L06501. https://doi.org/10.1029/2012GL050874

Steele, M., & Dickinson, S. (2016). The phenology of Arctic Ocean surface warming. *Journal of Geophysical Research: Oceans*, *121*, 6847–6861. https://doi.org/10.1002/2016JC012089

Stroeve, J., Kattsov, V., Barrett, A., Serreze, M., Pavlova, T., Holland, M., & Meier, W. N. (2012). Trends in Arctic sea ice extent from CMIP5, CMIP3 and observations. *Geophysical Research Letters*, *39*, L16502. https://doi.org/10.1029/2012GL052676

Stroeve, J., Markus, T., Boisvert, L., Miller, J., & Barrett, A. (2014). Changes in Arctic melt season and implications for sea ice loss. *Geophysical Research Letters*, *41*, 1216–1225. https://doi.org/10.1002/2013GL058951

Timmermans, M.-L., Toole, J., & Krishfield, R. (2018). Warming of the interior Arctic Ocean linked to sea ice losses at the basin margins. *Science Advances*, *4*(8), eaat6773.

Walsh, J. E., Chapman, W. L., Fetterer, F., & Stewart, J. S. (2019). *Gridded monthly sea ice extent and concentration, 1850 onward, version 2*. Boulder, CO: NSIDC: National Snow and Ice Data Center. https://doi.org/10.7265/jj4s-tq79

Wang, M., & Overland, J. E. (2015). Projected future duration of the sea-ice-free season in the Alaskan Arctic. *Progress in Oceanography*, *136*, 50–59.

Wassmann, P., Duarte, C. M., Agusti, S., & Sejr, M. K. (2011). Footprints of climate change in the Arctic marine ecosystem. *Global Change Biology*, *17*(2), 1235–1249.